

Article

“*Candidatus Mystax nordicus*” Aggregates with Mitochondria of Its Host, the Ciliate *Paramecium nephridiatum*

Aleksandr Korotaev ^{1,†}, Konstantin Benken ²  and Elena Sabaneyeva ^{1,*} 

¹ Department of Cytology and Histology, Saint Petersburg State University, 199034 Saint Petersburg, Russia; aleksandr.korotaev@unibas.ch

² Core Facility Centre for Microscopy and Microanalysis, Saint Petersburg State University, 199034 Saint Petersburg, Russia; cbenken@gmail.com

* Correspondence: e.sabaneeva@spbu.ru

† Current address: Focal Area Infection Biology, Biozentrum, University of Basel, 4056 Basel, Switzerland.

Received: 10 May 2020; Accepted: 16 June 2020; Published: 19 June 2020



Abstract: Extensive search for new endosymbiotic systems in ciliates occasionally reverts us to the endosymbiotic bacteria described in the pre-molecular biology era and, hence, lacking molecular characterization. A pool of these endosymbionts has been referred to as a hidden bacterial biodiversity from the past. Here, we provide a description of one of such endosymbionts, retrieved from the ciliate *Paramecium nephridiatum*. This curve-shaped endosymbiont (CS), which shared the host cytoplasm with recently described “*Candidatus Megaira venefica*”, was found in the same host and in the same geographic location as one of the formerly reported endosymbiotic bacteria and demonstrated similar morphology. Based on morphological data obtained with DIC, TEM and AFM and molecular characterization by means of sequencing 16S rRNA gene, we propose a novel genus, “*Candidatus Mystax*”, with a single species “*Ca. Mystax nordicus*”. Phylogenetic analysis placed this species in Holosporales, among *Holospora*-like bacteria. Contrary to all *Holospora* species and many other *Holospora*-like bacteria, such as “*Candidatus Gortzia*”, “*Candidatus Paraholospora*” or “*Candidatus Hafkinia*”, “*Ca. Mystax nordicus*” was never observed inside the host nucleus. “*Ca. Mystax nordicus*” lacked infectivity and killer effect. The striking peculiarity of this endosymbiont was its ability to form aggregates with the host mitochondria, which distinguishes it from *Holospora* and *Holospora*-like bacteria inhabiting paramecia.

Keywords: symbiosis; *Paramecium*; ciliates; *Holospora*-like bacteria; host–parasite interactions; 16S rRNA gene; full-cycle rRNA approach; TEM; fluorescence in situ hybridization

1. Introduction

The ability of ciliates to form symbiotic associations with other microorganisms is well known [1–5]. Phagocytosis makes these protists predisposed to various infections, especially bacterial ones [6]. With intensification of sampling worldwide, the number of novel endosymbiotic bacteria discovered in ciliates is growing year by year [7–13]. Endosymbiotic systems in ciliates have long been studied in light of their importance in ecological systems and evolutionary impact [14–19]. Besides that, presumably the ancient origin of such associations enables using ciliate symbiotic systems as models for studying the evolution of early endosymbiosis of a protoeukaryote and the mitochondrial ancestor, which lay at the core of modern biodiversity [20]. Moreover, some recent findings support the hypothesis that ciliates, like some other protists, can harbor microbes potentially pathogenic for humans or economically significant animals [21–25]. Interestingly, endosymbiotic bacteria seem to be more frequent in the ciliate

species found in brackish water habitats, which might be connected with the ability of endosymbiotic bacteria to promote expansion of salinity tolerance in ciliates [26–28].

Extensive search for new endosymbiotic systems in ciliates occasionally reverts us to the endosymbionts described in the pre-molecular biology era, which lacked molecular techniques. Consequently, many of about 60 endosymbionts registered in *Paramecium* and beyond [29] had been described only morphologically and, therefore, are out of the scope of modern molecular phylogenetics. A pool of these endosymbionts, which are nowadays being rediscovered, for example, *Lyticum flagellatum* and *L. sinuosum* [30], as well as “*Candidatus* Trichorickettsia mobilis” [18], has been referred to as a hidden bacterial biodiversity from the past [7] (p. 1017).

For a long time, *Paramecium nephridiatum* has been considered an uncertain species [31]. It was rediscovered and described as a true morphospecies only in 1999 [32]. A number of bacterial endosymbionts have been found in the population of *P. nephridiatum*, at the time misidentified as *P. woodruffi*, isolated from a tidepool on the Sredniy Island (Chupa Inlet, the White Sea) [29,33]. The morphology of three types of cytoplasmic bacteria has been described; however, their phylogenetic position has remained unclear, and two of them have not been given binomial names. The third one was described as *Pseudolyticum minutus* [33]. Nearly 30 years later, sampling in the same tidepool, we isolated a population of *P. nephridiatum* seemingly bearing the same set of endosymbionts. Here we provide a morphological and molecular characterization of two of these previously described cytoplasmic endosymbionts of *P. nephridiatum*, one of which we propose to name “*Ca. Mystax nordicus*”, gen. nov., sp. nov., based on its appearance and geographic origin of the isolate.

2. Materials and Methods

2.1. Cell Cultures and Live-Cell Experiments

Paramecium strains BMS16-23, BMS16-34 and BMS17-1 were isolated in 2016 and 2017, respectively, from a population of *Paramecium* cells found in a brackish water pool in the littoral zone of the Sredniy island the White Sea, Russia (66°16′59.2″ N 33°42′29.2″ E). Cells of all three strains carried infection in their cytoplasm and were subjected to further investigation. A naïve *P. nephridiatum* strain, ETu5-1, maintained at RC CCM Culture Collection (Core Facility Center for Cultivation of Microorganisms) and kindly provided by N. A. Lebedeva, was used in experimental infections as well as in killer trait assessments. The cells were grown at 16 °C in boiled lettuce medium inoculated with *Klebsiella aerogenes*. Live-cell observations were made with a compression device [34] and a Leica 6000B microscope (Leica Microsystems, GmbH, Wetzlar, Germany) equipped with differential interference contrast (DIC) and a digital camera DFC500.

2.2. Killer-Trait Assessment and Experimental Infection

Killer tests were carried out as follows: 20 cells of the infected BMS17-1 strain were mixed with 10 *Paramecium* cells of ETu5-1 strain in a depression slide containing approximately 500 µL of cultivation medium. The number of living and motile cells was counted after 30 min, 60 min and 24 h.

The experimental infections were performed with homogenate made of infected BMS17-1 cells. The infected cells were washed several times with sterile lettuce medium and concentrated. Then the cells were homogenized using a syringe with a thin needle. The amount of the homogenate added to 20 naïve ETu5-1 cells was calculated as a 1:10 ratio of naïve to infected cells. A drop of medium containing food bacteria was added to stimulate phagocytosis. The efficiency of the infection was checked in 1.5 and 72 h after the start of the experiment with FISH.

2.3. Transmission Electron Microscopy (TEM)

Paramecia were fixed in phosphate buffer (0.1 M, pH 7.4) containing 1.6% paraformaldehyde and 2.5% glutaraldehyde for 1.5 h at room temperature as described by Szokoli and colleagues [35]. Then the cells were washed in the same buffer containing 12.5% sucrose and postfixed in 1.6% OsO₄

(1 h at 4 °C). After that, the cells were dehydrated in ethanol gradient followed by ethanol/acetone mixture (1:1), 100% acetone and embedded in Epoxy embedding medium (FlukaChemie AG, St. Gallen, Switzerland) according to the manufacturer's protocol. The blocks were sectioned with a Leica EM UC6 Ultracut, and ultrathin sections were stained with aqueous 1% uranyl acetate followed by 1% lead citrate. All samples were examined with a JEM-1400 electron microscope (JEOL Ltd., Tokyo, Japan) at 90 kV.

Negative staining was performed to test for the presence of flagella on the symbiont surface. For this purpose, the host cells were washed several times with sterile lettuce medium, incubated in it for 24 h and then washed again before the sample preparation. Several cells were squashed, and a drop of the resulting suspension was transferred to a Formvar coated grid. The bacteria were allowed to precipitate for about 1 min, and then the grid was covered with 1% uranyl acetate in water for about 1 min. Then the liquid was removed with filter paper, and the grid was air-dried.

2.4. Atomic Force Microscopy (AFM)

A few live *Paramecium* cells were washed several times with sterile lettuce medium, incubated in it for 24 h and then washed again before the sample preparation. Then they were placed on a coverslip in a small drop of the sterile medium and ruptured with a needle. The contents of the ruptured cell were air-dried. The material was examined using NTEGRA Aura (NT MDT, Russia) in a semi-contact mode.

2.5. Molecular Characterization

For total DNA extraction, approximately 100 cells were washed several times with sterile lettuce medium and fixed in 70% ethanol. The cells were homogenized with a syringe in 50 mM EDTA solution to inhibit DNA degradation by DNases in cell lysate. Total DNA was extracted with NucleoSpin®Plant DNA Extraction Kit (Macherey-Nagel GmbH & Co., Düren NRW, Germany) using the protocol for fungal DNA extraction.

The host species were preliminarily identified using morphological features [36], and their attribution was subsequently confirmed by sequencing 18S rRNA gene following the approach suggested by Petroni and colleagues [37]. The amplification of the host 18S rRNA genes from total DNA was performed with the 18S_F9 [38] and 18S R1513Hypo primers (Table S1) [37]. PCR products were directly sequenced with 18S_F9 and R1513Hypo or 18S_R536, 18S_F783, 18S_F919 and 18S_R1052 (Table S1) [39].

For molecular characterization of bacterial endosymbionts, almost the full 16S rRNA gene was amplified with the 16S_αF19b and 16S_R1522a primers (Table S1) [40]. The touchdown PCR protocol described by Szokoli and colleagues [35] was employed with modifications, and Thermo Scientific InsTAclone PCR Cloning Kit (Thermo Scientific, USA) was used for molecular cloning. Amplification products were cloned into the pTZ57R/T vector and transformed into competent JM107 *Escherichia coli* cells following the manufacturer's instructions. Bacterial colonies were used for colony PCR with M13 primers. PCR products were sequenced using M13 primers and 16S_R1488_Holo [30], 16S_F343ND, 16S_R515ND and 16S_F785ND (Table S1) [40].

2.6. Fluorescence in Situ Hybridization (FISH)

To verify that the obtained 16S rRNA gene sequences were derived from the endosymbiotic bacteria, specific fluorescent oligonucleotide probes were designed: 16S_Myst965 (5'-CCT GTA CTA AAT CGG CCG AAC CG-3') and 16S_MegVen1226 (5'-CCG AAC TGA GAT GCC TTT TGAG-3') which were labeled with either Cy3 or FAM at the 5' end. The probes were synthesized and labeled with fluorescent dyes by Evrogen (Moscow, Russia). The newly designed probes were tested at 0%, 15% and 30% formamide (FA) concentrations. Their specificity was determined in silico using the tools TestProbe 3.0 (SILVA rRNA database project) [41] and the ProbeMatch of the Ribosomal Database Project (RDP) [42], allowing 0 mismatches. All FISH experiments were performed as described by Manz and colleagues [43]. The designed probes were used in combination with the almost universal eubacterial

probe Eub338 (5'-FAM-GCT GCC TCC CGT AGG AGT-3') labeled with FAM at the 5' end [44]. The slides were mounted in Mowiol (Calbiochem, Germany) containing PPD (p-phenylenediamine) and DAPI prepared according to manufacturer's protocol. The slides were analyzed with a Leica TCS SPE Confocal Laser Scanning Microscope (CLSM).

2.7. Phylogenetic Analysis

A total of 63 sequences of 16S rRNA genes were used for reconstruction of phylogeny. Among them, 5 sequences of distant relatives of Alphaproteobacteria and 8 sequences originating from 4 different classes of Proteobacteria (Epsilon-, Delta-, Beta- and Gamma-) were used as an outgroup. All the sequences were aligned with SSU-ALIGN 0.1.1 software and masked using default settings [45]. For the selection of model of nucleotide substitution, jModelTest2.1 was employed, and GTR+I+G model was chosen [46]. Phylogenetic analysis was performed with PhyML 3.1 with 1000 pseudo-replicates [47]. The final tree was visualized with FigTree v1.4.3 [48].

2.8. Accession Numbers

The sequences of 16S and 18S rRNA genes were submitted to NCBI GenBank and were assigned accession numbers MK764889 and MK764894 (*P. nephridiatum*); MK775140 and MK775139 ("*Ca. Megaira venefica*"); MK673804 ("*Ca. Mystax nordicus*").

3. Results

3.1. Host Identification

Identification of the host species was based on morphological and molecular features that included cell size, number of micronuclei and pores, structure of contractile vacuoles and the sequence of 18S rRNA gene. For morphological identification, we employed the key to the main morphospecies made by Fokin [36]. *Paramecium* cells of BMS16-23, BMS16-34 and BMS17-1 strains were preliminarily identified as *P. nephridiatum*, which is characterized as a 150–200 µm long cell, containing 2–6 micronuclei and from 2 to 5 pores of contractile vacuoles [36]. Subsequently, morphological identification was confirmed by direct sequencing of 18S rRNA gene amplified fragments of BMS16-23 and BMS16-34 cells. The obtained sequences (1748 bp and 1640 bp, accession numbers MK764889 and MK764894, respectively) showed 99–100% identity (NCBI GenBank) to the sequences of *P. nephridiatum* (MG573198.1, [49]; HE978251.1, [50]) and one sequence of *P. duboscqui* (HM140398.1; reference unpublished). Given clear morphological differences between these two species [36] and morphological similarity of the ciliates of our strains and *P. nephridiatum*, the obtained sequences were annotated as corresponding to the species *P. nephridiatum*. Interestingly, the comparison of the HM140398.1 sequence to other 18S rRNA of *P. duboscqui* showed only ~93% similarity implying that, apparently, the sequence HM140398.1 must have been derived from *Paramecium* species misidentified as *P. duboscqui*.

3.2. Morphology and Biology of the Endosymbionts

Two morphologically unlike bacterial endosymbionts were found in the BMS population of *Paramecium* (Figure 1). Two morphotypes could be easily distinguished on the basis of their morphology. The endosymbionts of the first morphotype were curve-shaped (CS), 0.6–0.8 µm wide and 4–7 µm long (Figure 1A,B). In turn, the bacteria of the second morphotype were rod-shaped (RS), 0.4–0.5 µm wide and 1.1–2.5 µm long (Figure 1C). Both CS- and RS-endosymbionts formed a triple symbiotic association (CS + RS + host) in cells of BMS16-23 and BMS17-1 strains, while the strain BMS16-34 harbored only RS-endosymbionts, thus representing a double symbiotic system.

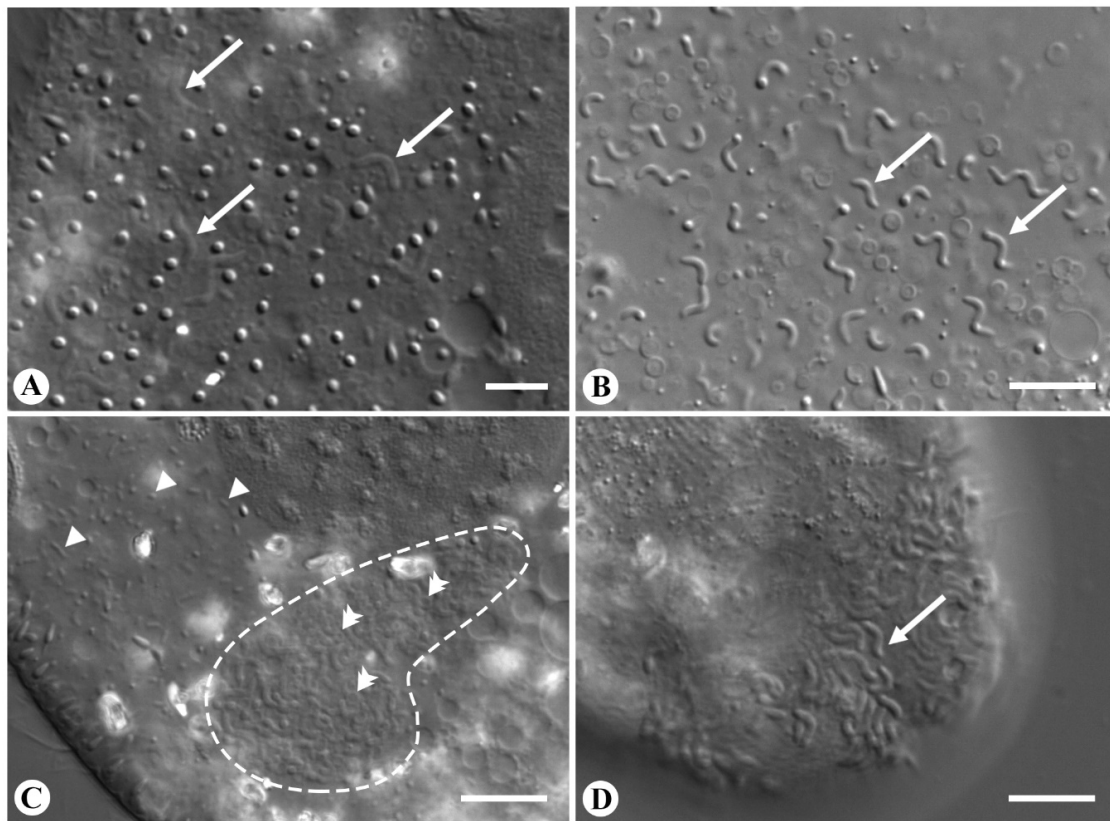


Figure 1. Curve-shaped (CS)-bacteria from the cytoplasm of *P. nephridiatum* strains BMS16-23, BMS17-1, DIC; (A) a fragment of the living cell cytoplasm; white arrows point to CS-bacteria in the cytoplasm; (B) bacteria released from a squashed cell (arrows); (C) a fragment of the intact cell cytoplasm; the outlined area encloses a bacterial cluster consisting of CS-bacteria, white arrowheads point to rod-shaped (RS)-bacteria; double arrowheads point to structures resembling mitochondria; (D) the surface of the intact cell; white arrow points to the bacteria attached to the paramecia. Scale bar 5 μm (A), 10 μm (B–D).

The CS-bacteria often formed clearly visible clusters in living host cells (Figure 1C). Apart from CS-endosymbionts, these clusters comprised host cytoplasm structures resembling mitochondria. In rare cases of hyperinfected cells, CS-bacteria were found sticking out of the cortex of the host cell (Figure 1D). However, it remains elusive whether this is a sophisticated mechanism of egress from the host cell or a consequence of cell overpopulation resulting in disintegration of the host pellicle. Microscopy of living and squashed host cells showed no motility of CS-bacteria, either in cytoplasm of a host cell or in cultivation medium. In contrast, RS-bacteria demonstrated fast chaotic movements both inside and outside of host cells resembling continuous tumbling motility.

The prevalence for both endosymbionts was 100% at the start of the laboratory culture; however, the number of CS-symbionts per host cell in BMS16-23 gradually decreased over time, and eventually, these endosymbionts were lost. Further work was continued using BMS17-1 strain. Nevertheless, by the end of the second year of cultivation, the prevalence for CS-symbionts in BMS17-1 also reduced to about 10% or less, and these symbionts seemed to have been lost in this strain as well. However, checking the culture over time revealed several ciliates still infected with CS-endosymbiont. Thus, the infection persists, though at a very low prevalence. During 2 years of observations, we regularly observed the fluctuations of both the prevalence and of the endosymbiont load per cell. On the contrary, the prevalence of RS-bacteria did not change with time in any of the three strains. Both endosymbionts resided exclusively in the cytoplasm and were never observed in nuclei or other compartments throughout the whole period of cultivation.

Killer-trait assay of BMS17-1 endosymbionts did not show any decrease in the naive cell number that would indicate a killer effect. However, no mating was done to exclude mate-killing ability.

In our experiments, neither of the endosymbionts demonstrated any infectious capacity.

3.3. Fine Structure of the Endosymbionts

In TEM sections, the CS-symbionts showed the typical morphology of Gram-negative bacteria. The bacteria were not surrounded by an additional host membrane and lay "naked" in the cytoplasm (Figure 2A). The cytoplasm of CS-symbionts had moderate electron density with conspicuous ribosomes and free electron-lucid areas (Figure 2A).

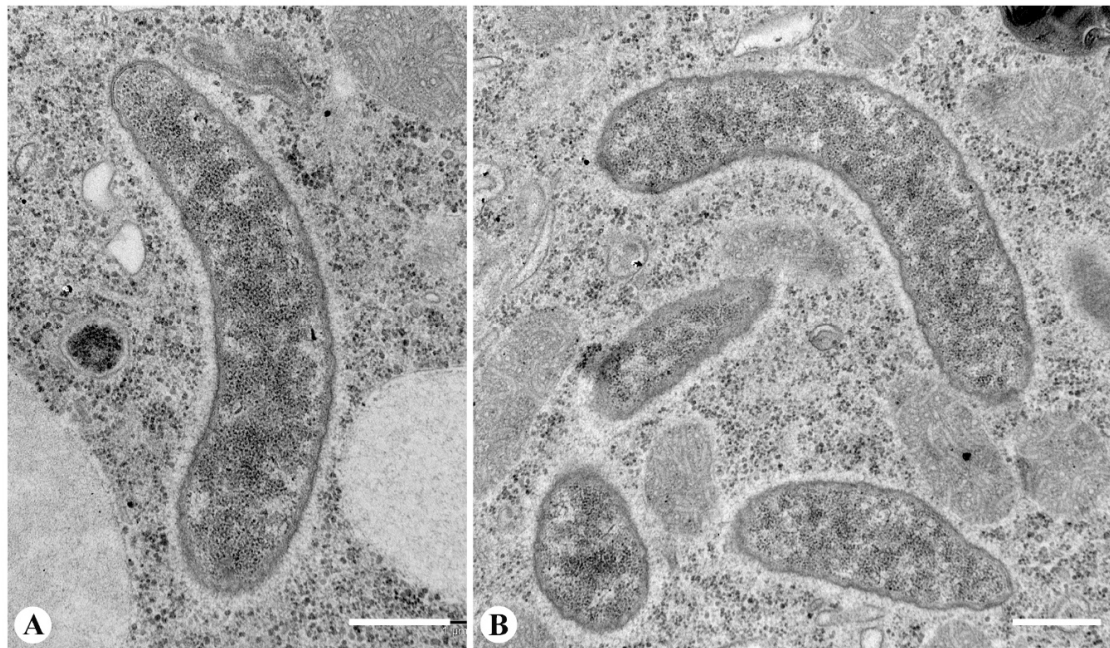


Figure 2. Transmission electron microscopy images of CS-bacteria in the cytoplasm of *P. nephridiatum* strain BMS16-23. (A) The bacterium in the cytoplasm. (B) A fragment of a putative conglomeration with the host mitochondria. Scale bar 500 nm.

No other morphological structures were registered (Figure 2). In order to confirm our observations made with TEM, we examined the surface of bacteria with AFM (Figure 3). The images obtained with AFM did not show any structures on the bacterial surface, like flagella or an invasion tip, a peculiar feature typical for the infectious forms of *Holospira* [51] and other representatives of *Holosporales*, "*Ca. Gortzia*" and *Preeria* [9,52,53], which is thought to be crucial for the infection process of naive host cells in these species. It is noteworthy that the bacteria were often located close to mitochondria; however, direct contact of membranes was never observed (Figure 2B, Figure S1). This finding is consistent with live-cell observations and suggests that CS-bacteria tend to form clusters with mitochondria.

In contrast, the RS-bacteria were randomly distributed in the cytoplasm and never formed conglomerates with CS-symbionts or host cell organelles. In electron micrographs, RS-endosymbionts demonstrated two typical membranes of Gram-negative bacteria (Figure 4A). The cytoplasm was electron-dense and homogeneous without any inclusions. Bacterial cells were not enclosed by any additional membrane and were always surrounded by electron-lucid host cytoplasm lacking ribosomes. No flagella were observed in fine sections, however, negatively stained RS-bacteria showed moderate flagellation (up to seven flagella) (Figure 4B), which was confirmed by probing bacterial surface with AFM (Figure S2). The flagella were evenly distributed all over the bacterial surface, implying a peritrichous type of flagellation.

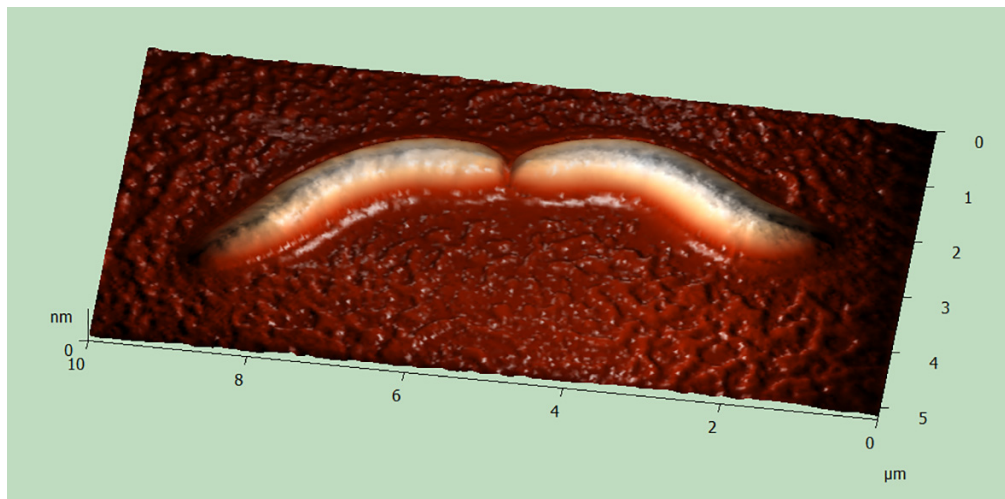


Figure 3. 3D reconstruction of CS-bacterium released from the cytoplasm of *P. nephridiatum* strain BMS16-23, AFM.

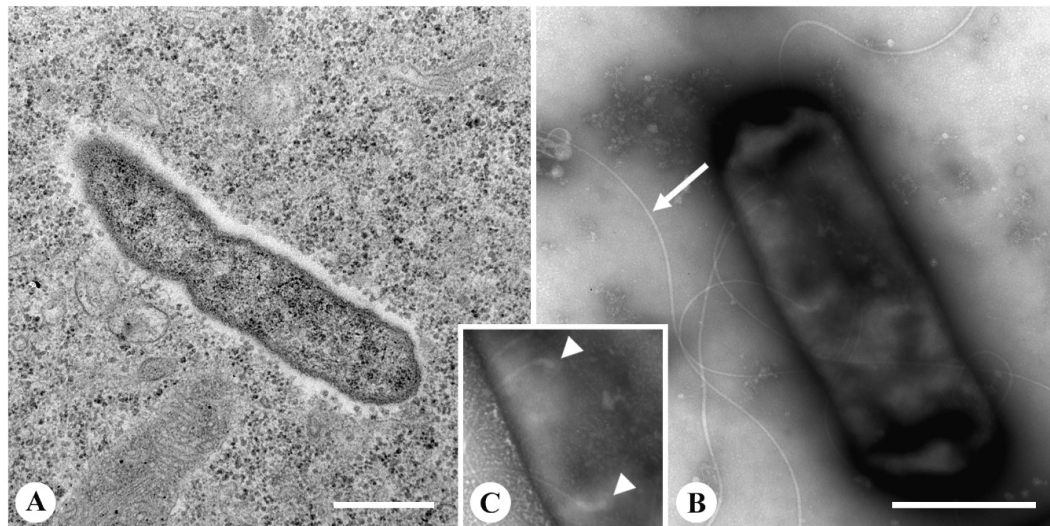


Figure 4. Transmission electron microscopy images of RS-bacteria in the cytoplasm of *P. nephridiatum* strain BMS16-34; (A) the bacterium in the cytoplasm; (B) the moderately flagellated bacterium cell, negative staining; white arrow points to the flagellum; (C) an enlarged fragment of bacterium surface; white arrowheads point to the hooks and l-rings. Scale bar 500 nm.

3.4. Molecular Characterization of the Endosymbionts

Nearly full-length sequences of 16S rRNA gene of endosymbionts of BMS16-23 (CS-symbiont: 1479 bp, accession number MK673804; RS-symbiont: 1478 bp, MK775140) and BMS16-34 (RS-symbiont: 1479 bp, MK775139) strains were obtained and compared with the data available from NCBI GenBank. The sequences of RS-bacteria from two strains were 99% similar and showed the highest identity score (99–100%) with the sequences of “*Ca. Megaira venefica*” (MG563925.1, MG563928.1) that has been described recently [49]. The highest sequence identity (95%) of CS-symbionts was observed with another *Paramecium* endosymbiont “*Ca. Paraholospira nucleivisitans*” (EU652696.1) [54]. Based on the obtained sequences, species-specific, fluorescently labeled oligonucleotide probes (16S_Myst965 for CS-symbionts and 16S_MegVen1226 for RS-bacteria (Table S1)) were designed to verify that the obtained sequences belonged to the endosymbionts (CS- and RS-bacteria, correspondingly) residing in the cells of BMS16-23, BMS16-34 and BMS17-1 strains. The designed probes were employed together with the Eub338 probe and were tested in FISH experiments at 0%, 15% and 30% formamide

concentrations. The 16S_Myst965 probe showed specific hybridization with CS-symbionts at all formamide concentrations. Binding of the 16S_MegVen1226 probe to 16S rRNA of RS-symbionts was observed at 0% and 15%, but not at 30% concentration of formamide. Surprisingly, the 16S_MegVen1226 probe revealed non-specific labeling of CS-symbionts at 0% and 15% formamide. Increasing formamide concentration up to 20% led to specific labeling of the RS-symbionts only. Mapping the 16S_MegVen1226 nucleotide probe to 16S rRNA gene sequence of BMS16-23 cells revealed that they share 17 of 22 nucleotides of the probe, which accounts for non-specific binding.

The FISH results demonstrated exclusively cytoplasmic localization of both endosymbionts (Figure 5). In accordance with live-cell observations and TEM images, CS-bacteria showed non-random distribution in the cytoplasm forming clusters and occasional location underneath the host cell membrane (Figure 5A–C). The bacterial load in a cell varied substantially from single cells to multiple cell clusters located throughout the whole cytoplasm (Figure 5). Moreover, bacteria penetrating the cortex were observed in some heavily infected ciliates (Video S1). On the contrary, RS-bacteria seemed to be uniformly distributed in the cytoplasm (Figure 5C,D).

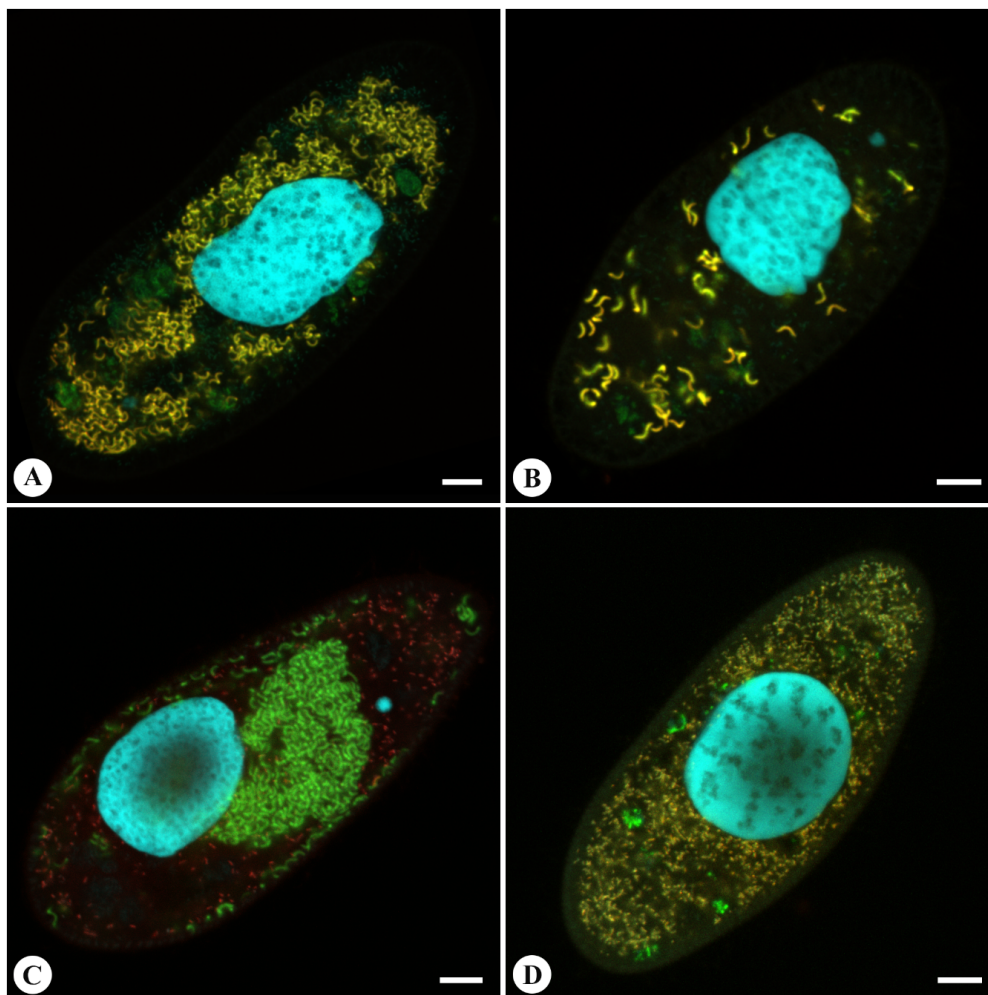


Figure 5. Fluorescent in situ hybridization of the endosymbionts in cells of *P. nephridiatum*, Confocal Laser Scanning Microscope (CLSM); (A,B) BMS16-23 and BMS17-1 cells labeled with 16S_Myst965 probe (red) and the universal eubacterial probe Eub338 (green) counterstained with DAPI (cyan), FA concentration 15% and 30%, respectively; (C) BMS17-1 cells labeled with 16S_MegVen1226 (red) and 16S_Myst965 (green) probes counterstained with DAPI (cyan), FA concentration 20%; (D) BMS16-34 cells labeled with 16S_MegVen1226 (red) and the universal eubacterial probe Eub338 (green) counterstained with DAPI (cyan), FA concentration 0%. Scale bar 10 μ m.

Phylogenetic reconstructions covering 63 sequences of 16S rRNA gene including two sequences corresponding to identified RS- and CS-bacteria were made (Figure 6). The sequence of RS-symbiont formed a well-supported monophyletic clade with sequences of “*Ca. Megaira venefica*” and “*Ca. Megaira polyxenophila*” and formed one defined clade with sequences of pathogens *Rickettsia* and symbionts “*Ca. Trichorickettsia*” and “*Ca. Gigarickettsia*”, order Rickettsiales. In turn, the sequence of CS-symbiont grouped with representatives of order Holosporales. In particular, it formed a branch distant to the core *Holospora* spp. and standing apart, like the sequences of other orphan taxa *Preeria caryophila* [53], “*Ca. Paraholospora nucleivisitans*” [54], and “*Ca. Bealeia paramacronuclearis*” [55]. Within this clade, CS-symbiont showed closer relation to another *Paramecium* endosymbiont “*Ca. Paraholospora nucleivisitans*”. Of note, the *Holospora*-like bacteria tending to associate with the host energy organelles taken into analysis (“*Ca. Cytomitobacter*” spp., “*Ca. Hydrogenosomobacter endosymbioticus*” and the CS-symbiont, which we propose to name “*Ca. Mystax nordicus*”) form separate clades in the phylogenetic tree, suggesting that the affinity to the host energy organelles may have originated independently.

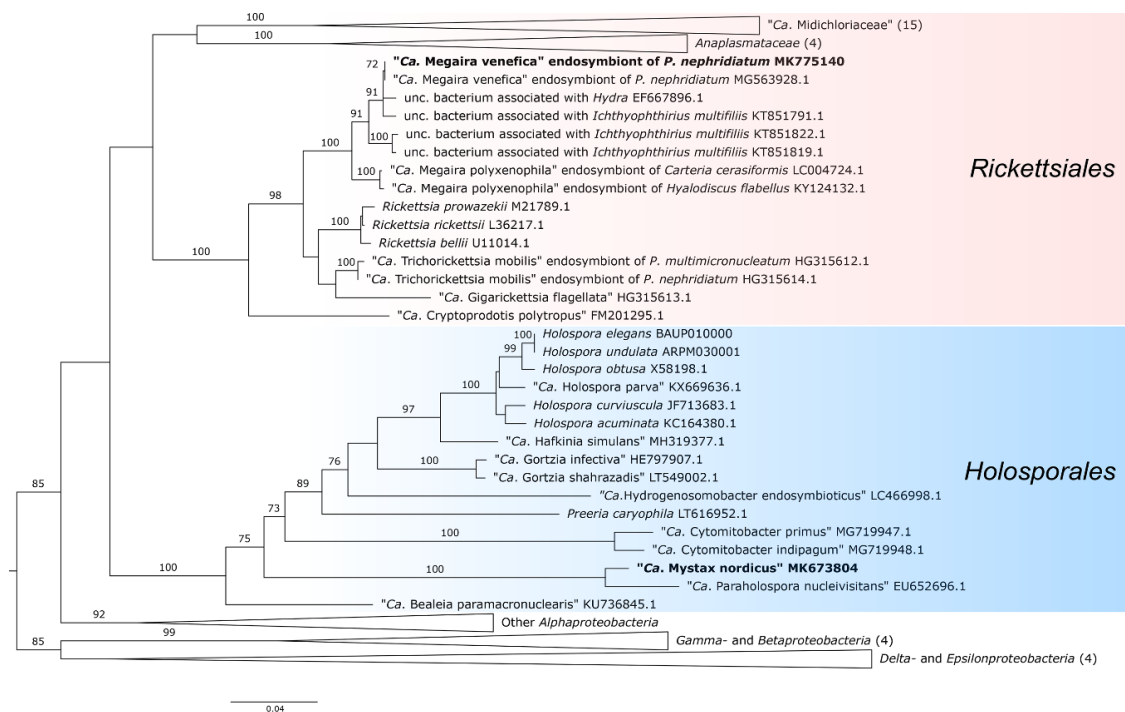


Figure 6. Maximum likelihood phylogenetic tree of 63 sequences inferred on 1399 16S rRNA gene nucleotide positions with the GTR+I+G substitution model. Reported in bold are sequences characterized in this study. Numbers associated with each node correspond to maximum likelihood bootstrap values (values below 70% are omitted); numbers in brackets indicate the number of sequences representing that clade. The bar stands for an estimated sequence divergence of 4%. Abbreviations: *Ca.*—Candidatus; unc.—uncultured.

4. Discussion

4.1. RS- and CS-Bacteria Are Endosymbionts from the Past

Here we provide morphological and molecular description of the two bacterial endosymbionts from the cytoplasm of *P. nephridiatum*, RS- and CS-bacteria. These endosymbionts show morphological and ecological similarity to symbionts from the past, first identified by Fokin in 1989 as endobionts 1 and 3 (Eb1 and Eb3 respectively) [33], retrieved in the same species in the same sampling spot. 16S rRNA gene of RS-bacteria showed 99–100% sequence similarity to that of “*Ca. Megaira venefica*”, which has been described recently from the same ciliate species from the same location [49]. In the latter

study, “*Ca. Megaira venefica*” from *P. nephridiatum* has not been shown to possess any flagella, though in other hosts, such as *Paramecium bursaria*, structures resembling flagella have been occasionally revealed. Until recently, bacteria of order *Rickettsiales* have been thought to be devoid of flagella and flagella-mediated movement [56]. However, new findings have appeared, showing the inaccuracy of that statement [18,20,30]. Initially, flagella traces were found as a set of *fli*-genes in the genome of “*Ca. Midichloria mitochondrii*” [20], and later heavily flagellated endosymbionts *Lyticum* sp. [30], “*Ca. Trichorickettsia mobilis*” and “*Ca. Gigarickettsia flagellate*” [18] were identified in ciliates *Paramecium* spp. Here we provide direct evidence showing the presence of flagella in another paramecia endosymbiont “*Ca. Megaira venefica*” [49]. Although “*Ca. Megaira venefica*” has been shown to have the structures resembling flagella in one of the host species, the data were not conclusive. We demonstrated the presence of rare flagella (up to seven flagella) distributed over the whole bacterial surface. Similarly to Lanzoni and colleagues [49], we were not able to notice any substantial signs of flagella in TEM images, which could be explained by the low thickness of fine sections and a few flagella presented on the surface of bacteria.

By its size and morphology, the curved endosymbiont (CS) retrieved from the cytoplasm of *P. nephridiatum* resembles one of the endobionts (Eb3) isolated from the same place about 30 years ago [33]. Both of them are curved, and their dimensions are $4\text{--}7 \times 0.6\text{--}0.8 \mu\text{m}$ for CS in our study, and $3.5\text{--}7 \times 1.2\text{--}1.3 \mu\text{m}$ for Eb3 according to the study of 1989 [33]. In both studies, bacteria did not show any motility. The appearance of living bacteria in DIC images is very similar. The only significant difference is the presence of the host cell membrane encircling the bacterium in the TEM image provided by Fokin [33]. However, the vast space of the vacuole, the thickness of its membrane, and the appearance of the bacterium enclosed cause some doubts concerning the function of the vacuole. It might be considered an autophagosome, rather than a symbiontophorous vacuole. In support of this idea is the TEM image presented by Fokin [33], which shows the vacuole to contain the fragment of the host cell cytoplasm alongside the bacterium, suggesting disposal of parts of the cytoplasm. In addition, in Fokin’s study, high endosymbiont load (up to 100 bacteria) has been shown to be detrimental for the host cells, while our observations demonstrated that ciliates were viable even in the case of much higher bacterial load, which might be explained as a result of endosymbiont adaptation to the host or more favorable cultivation conditions. Despite the presence of these discrepancies, taking into account the dimensions, the shape, the general appearance and the identical host species, we suggest the identity of Eb3 and CS-symbiont.

4.2. Phylogeny and Taxonomy

The sequence of 16S rRNA gene of the CS-symbiont demonstrated the highest proximity to the endosymbiont of *Paramecium sexaurelia* “*Ca. Paraholospora nucleivisitans*” [54]. According to Yarza et al. the minimum and median identity values to delineate bacterial genera are 94.5% and 96.4%, correspondingly, though it is 94.5% similarity of 16S rRNA genes that is most commonly used to delineate representatives of one or two different genera [57]. Along these lines of reasoning, CS-symbionts are at the border with the genus “*Ca. Paraholospora*” as their sequence similarity is 95%. Recent analysis has shown that at least in some taxa (e.g., Bacillaceae [*Bacillus*]), the 16S rRNA gene identity minimum threshold value of 94.5% could underestimate genera diversity [58]. Thus, we are inclined to propose a new genus, “*Ca. Mystax*” with a single species “*Ca. Mystax nordicus*,” taking into account the following considerations and basing on the bacterial shape and geographic origin.

“*Ca. Paraholospora nucleivisitans*” is a curve-shaped endosymbiont of *Paramecium sexaurelia* standing apart in the phylogenetic tree, which demonstrates a unique trait of shuttling between two host cell compartments: cytoplasm and macronucleus [54]. Although “*Ca. Mystax nordicus*” has the same curved shape, the cell length is much shorter and endosymbionts exceeding $7 \mu\text{m}$ were never observed. Throughout two years of observations, CS-symbionts always resided in one host compartment, in the cytoplasm, and were never observed in the host nucleus, which distinguishes it from the most closely related *Holospora* and *Holospora*-like bacteria, except

“*Ca. Bealeia paramacronuclearis*”, which demonstrates affinity to the host macronucleus, but is never found inside it [55]. An important peculiarity of “*Ca. Mystax nordicus*” is its ability to aggregate with the host cell mitochondria. Besides that, in contrast to “*Ca. Paraholospora nucleivisitans*” residing in *P. sexaurelia*, which inhabits predominantly tropical and subtropical areas [59], “*Ca. Mystax nordicus*” was identified in *P. nephridiatum*, dwelling about 30 km from the Arctic Circle. As the endosymbionts incapable of living outside their host are restricted to the host habitat, differences in the latter suggest that “*Ca. Paraholospora nucleivisitans*” and “*Ca. Mystax nordicus*” might have different temperature optimums.

4.3. Biological Peculiarities of “*Ca. Mystax nordicus*”

“*Ca. Mystax nordicus*” lacks a life cycle typical of *Holospora* and “*Ca. Gortzia*”, comprising a reproductive and an infectious form. The infectious form responsible for the horizontal spread of these endosymbionts is equipped with an infectious tip—a morphological structure on a bacterial pole that is thought to play a crucial role in the infection. The absence of the infectious tip, demonstrated by both TEM and AFM, supports the results of our experimental infections. Contrary to “*Ca. Paraholospora nucleivisitans*” shuttling between the cytoplasm and the nucleus [54] and “*Ca. Gortzia shahrazadis*” occasionally found in the cytoplasm [9], “*Ca. Mystax nordicus*” never occurred in the nucleus throughout two years of cultivation. Nuclear location is believed to be a prerequisite for differentiation of infectious forms in *Holospora* and *Holospora*-like bacteria [51]. The absence of the infectious tip and the infectious capacity seems to correlate with the cytoplasmic location of the endosymbiont. To our knowledge, it is the intranuclear endosymbionts that are highly infectious.

One of the most remarkable features of “*Ca. Mystax nordicus*” distinguishing it from many other cytoplasmic endosymbionts, such as “*Ca. Fokinia*” [35], “*Ca. Bealeia*” [55], “*Ca. Megaira*” [49] and *Lyticum* [30], is the formation of aggregates that are potentially formed around mitochondria (Figure 1C, Figure 2B, Figure 5C and Figure S1). Since one of the main functions of mitochondria in a eukaryotic cell is the synthesis of energy supply in the form of ATP [60], it is tempting to suggest that “*Ca. Mystax nordicus*” might be directly using host mitochondria as energy factories. To our knowledge, this is the first report of putative interaction of mitochondria and endosymbionts observed in *Paramecia* spp. in situ. Our finding is in good agreement with the in silico studies [61]. Indeed, comparative genomic analysis of *Holospora* spp.—relatives of “*Ca. Mystax nordicus*” and another genus of endosymbionts from the family Holosporaceae infecting the ciliates of the genus *Paramecium*—has shown the absence of many biochemical pathways, e.g., citric acid cycle and glycolysis, and endosymbiont dependence on host energy supplies [61]. Interestingly, several other cases of more intimate mitochondria–endosymbiont interaction, when the bacterium resides in the host mitochondrion, have been reported for endosymbionts of another ciliate, *Spirostomum* [62], and tick *Ixodes* [63]. Additionally, “*Ca. Cytomitobacter primus*” has been recently registered invading mitochondria of the flagellate *Diplonema japonicum* [64]. Another example of endosymbiotic bacteria of ciliates associated with energy-producing organelles is “*Ca. Hydrogenosomobacter endosymbioticus*”, found adjacent to hydrogenosomes of its host, anaerobic scuticociliate *Trimyema compressum*, together with methanogenic archaea [65]. Besides the endosymbiont consumption of the host energy organelles’ metabolites, the host–endosymbiont interaction might also involve communication between the intracellular bacteria and the host mitochondria or hydrogenosomes. Recently, it has been hypothesized “that microbiome may affect the host by directly interacting with mitochondria through bacterial metabolites and specific signaling mechanisms” [66].

Endosymbiont number control and host sparing way of their egress from the host cell are believed to be characteristic of the evolutionary old endosymbiotic systems, while hyperinfection and rupture of the host cell membrane are typical for evolutionary young systems with unstable host–endosymbiont relations [67]. Along these lines of reasoning, profusion of “*Ca. Mystax nordicus*”, leading to the rupture of the host cell pellicle and, finally, to the host death, provides grounds for considering “*Ca. Mystax nordicus*” a recently acquired endosymbiont, as it poorly controls its number at least in the

laboratory conditions. However, this is rather surprising, taking into account the apparently vertical transmission of “*Ca. Mystax nordicus*”, since vertical transmission usually implies co-adaptation of the partners [68].

As was mentioned before, BMS16-23 and BMS17-1 cells represent the triple symbiotic association (CS + RS + host). Seemingly simultaneous occurrence of several endosymbionts in one host is much more common than was thought before [55]. It is assumed that the coexistence of two different endosymbionts in one host compartment is unstable and leads to survival of only one symbiont [28]. Nevertheless, these symbiotic systems could be maintained for almost 1.5 years. Only by the end of the second year “*Ca. Mystax nordicus*” was lost in both strains, while “*Ca. Megaira venefica*” remained in the host cytoplasm, which provides evidence for the more balanced interaction between the host and “*Ca. Megaira venefica*” than with “*Ca. Mystax nordicus*”. Our observations of non-viable host cells with “*Ca. Mystax nordicus*” sticking out of the host cortex support this suggestion. Thus, given all the morphological and biological peculiarities of the CS-endosymbionts, we propose to define the new genus “*Ca. Mystax*” with “*nordicus*” as the only species described so far.

4.4. Description of “*Candidatus Mystax nordicus*”

Mystax nordicus (‘Mys.tax ’nor.di.cus; L. masc. n. mystax, moustache—allusion to the symbiont shape, which resembles the gentleman’s mustache (Figure 3); L. adj. nordicus, northern, meaning that the symbiont and the host were found in northern latitudes). A large nonmotile curve-shaped bacterium; 0.6–0.8 µm wide and up to 7 µm long. Cytoplasmic endosymbiont of *P. nephridiatum*, forming conglomerations. Belongs to family Holosporaceae, order Holosporales. Basis of assignment: 16S rRNA gene sequence (accession number MK673804) and positive match with the specific FISH oligonucleotide probe 16S_Myst965 (5′-CCT GTA CTA AAT CGG CCG AAC CG-3′). Uncultured thus far.

5. Conclusions

Bacterial biodiversity from the past represents a pool of “hidden” bacteria identified in the previous research but poorly characterized by molecular techniques. We provided morphological and molecular description of two endosymbiotic bacteria inhabiting the cytoplasm of *Paramecium nephridiatum*, which resemble those identified 30 years ago. We complemented the description of one of the endosymbionts, recently described as “*Ca. Megaira venefica*” [49], by revealing moderate flagellation, the feature not very common within Rickettsiales. We characterized the second endosymbiont, which had a curved shape and tended to form aggregates with the host mitochondria. Based on morphology and 16S rRNA gene sequence a new taxon “*Ca. Mystax nordicus*” was proposed.

Supplementary Materials: The following are available online at <http://www.mdpi.com/1424-2818/12/6/251/s1>, Figure S1: TEM images of CS-bacteria in the cytoplasm of *P. nephridiatum* strain BMS16-23. A fragment of a putative conglomeration with the host mitochondria. Abbreviations: S—symbiont, M—mitochondria. Scale bar 2 µm. Figure S2: 3D reconstruction of RS-bacterium released from the cytoplasm of *P. nephridiatum* strain BMS16-34, AFM. White arrowheads point to the flagella. Table S1: Primers and FISH probes used in this study. Video S1: Animated FISH Z stack of the endosymbionts in *P. nephridiatum* strain BMS16-23, CLSM. Cells labeled with 16S_Myst965 probe (red) and counterstained with DAPI (cyan). White arrows point to the bacteria penetrating the cortex.

Author Contributions: Conceptualization, E.S.; data curation, A.K. and E.S.; funding acquisition, E.S.; investigation, A.K. and E.S.; supervision, E.S.; visualization, A.K., K.B. and E.S.; writing—original draft, A.K. and E.S.; writing—review and editing, A.K., K.B. and E.S. All authors have read and agreed to the published version of the manuscript.

Funding: This study was funded by RFBR, grant number 18-04-00562a to Elena Sabaneyeva.

Acknowledgments: The authors are grateful to Aisylu Shaidullina for her help with experimental infections. We would like to thank Natalia Lebedeva for providing the naive strain of ciliates from the RC CCM Culture Collection (Core Facility Centre “Cultivation of Microorganisms”). The study was performed using the equipment of Core Facility Centres of Saint-Petersburg State University “Microscopy and Microanalysis” and “Molecular and Cell Technologies”.

Conflicts of Interest: The authors declare no conflict of interest. The funders had no role in the design of the study; in the collection, analyses, or interpretation of data; in the writing of the manuscript, or in the decision to publish the results.

References

- Fenchel, T.; Perry, T.; Thane, A. Anaerobiosis and symbiosis with bacteria in free-living ciliates. *J. Protozool.* **1977**, *24*, 154–163. [[CrossRef](#)] [[PubMed](#)]
- Görtz, H.-D. Microbial infections in free-living Protozoa. *Crit. Rev. Immunol.* **2010**, *30*, 95–106. [[CrossRef](#)] [[PubMed](#)]
- Fokin, S.I. Frequency and biodiversity of symbionts in representatives of the main classes of Ciliophora. *Eur. J. Protistol.* **2012**, *48*, 138–148. [[CrossRef](#)]
- Schweikert, M.; Gortz, H.-D.; Fujishima, M. Symbiotic associations between Ciliates and prokaryotes. In *The Prokaryotes*, 4th ed.; Rosenberg, E., DeLong, E.F., Stackebrandt, E., Lory, S., Thompson, F., Eds.; Springer: Berlin/Heidelberg, Germany, 2013; Volume 1, pp. 427–463. [[CrossRef](#)]
- Castelli, M.; Sabaneyeva, E.; Lanzoni, O.; Lebedeva, N.; Floriano, A.M.; Gaiarsa, S.; Benken, K.; Modeo, L.; Bandi, C.; Potekhin, A.; et al. *Deianiraea*, an extracellular bacterium associated with the ciliate *Paramecium*, suggests an alternative scenario for the evolution of *Rickettsiales*. *ISME J.* **2019**, *13*, 2280–2294. [[CrossRef](#)] [[PubMed](#)]
- Gong, J.; Qing, Y.; Zou, S.; Fu, R.; Su, L.; Zhang, X.; Zhang, Q. Protist-bacteria associations: Gammaproteobacteria and Alphaproteobacteria are prevalent as digestion-resistant bacteria in ciliated protozoa. *Front. Microbiol.* **2016**, *7*, 498. [[CrossRef](#)] [[PubMed](#)]
- Fokin, S.; Serra, V. The Hidden Biodiversity of Ciliate-Endosymbionts Systems. *JSM Microbiol.* **2014**, *2*, 1015–1018.
- Lanzoni, O.; Fokin, S.; Lebedeva, N.; Migunova, A.; Petroni, G.; Potekhin, A. Rare freshwater ciliate *Paramecium chlorelligerum* Kahl, 1935, and its macronuclear symbiotic bacterium “*Candidatus Holospora parva*”. *PLoS ONE* **2016**, *11*, e0167928. [[CrossRef](#)]
- Serra, V.; Fokin, S.I.; Castelli, M.; Basuri, C.K.; Nitla, V.M.; Verni, F.; Sandeep, B.V.; Kalavathi, C.; Petroni, G. “*Candidatus Gortzia shahrazadis*”, a novel endosymbiont of *Paramecium multimicronucleatum* and revision of the biogeographical distribution of *Holospora*-like bacteria. *Front. Microbiol.* **2016**, *7*, 1704. [[CrossRef](#)]
- Senra, M.V.; Dias, R.J.; Castelli, M.; Silva-Neto, I.D.; Verni, F.; Soares, C.A.; Petroni, G. A house for two—Double bacterial infection in *Euplotes woodruffi* Sq1 (*Ciliophora*, *Euplotia*) sampled in Southeastern Brazil. *Microb. Ecol.* **2016**, *71*, 505–517. [[CrossRef](#)]
- Vannini, C.; Sigona, C.; Hahn, M.; Petroni, G.; Fujishima, M. High degree of specificity in the association between symbiotic betaproteobacteria and the host *Euplotes* (*Ciliophora*, *Euplotia*). *Eur. J. Protistol.* **2017**, *59*, 124–132. [[CrossRef](#)]
- Castelli, M.; Serra, V.; Senra, M.V.X.; Basuri, C.K.; Soares, C.A.G.; Fokin, S.I.; Modeo, L.; Petroni, G. The hidden world of *Rickettsiales* symbionts: “*Candidatus Spectririckettsia obscura*,” a novel bacterium found in Brazilian and Indian *Paramecium caudatum*. *Microb. Ecol.* **2018**, *77*, 748–758. [[CrossRef](#)] [[PubMed](#)]
- Fokin, S.; Serra, V.; Ferrantini, F.; Modeo, L.; Petroni, G. “*Candidatus Hafkinia simulans*” gen. nov., sp. nov., a novel *Holospora*-like bacterium from the macronucleus of the rare brackish water ciliate *Frontonia salmastra* (*Oligohymenophorea*, *Ciliophora*): Multidisciplinary characterization of the new endosymbiont and its host. *Microb. Ecol.* **2019**, *77*, 1092–1106. [[CrossRef](#)] [[PubMed](#)]
- Kusch, J.; Czubatinski, L.; Wegmann, S.; Hubner, M.; Alter, M.; Albrecht, P. Competitive advantages of *Caedibacter*-infected *Paramecia*. *Protist* **2002**, *153*, 47–58. [[CrossRef](#)] [[PubMed](#)]
- Gast, R.; Sanders, R.; Caron, D. Ecological strategies of protists and their symbiotic relationships with prokaryotic microbes. *Trends Microbiol.* **2009**, *17*, 563–569. [[CrossRef](#)]
- Nidelet, T.; Koella, J.C.; Koltz, O. Effects of shortened host life span on the evolution of parasite life history and virulence in a microbial host-parasite system. *BMC Evol. Biol.* **2009**, *9*, 65. [[CrossRef](#)]
- Nowack, E.; Melkonian, M. Endosymbiotic associations within protists. *Philos. Trans. R. Soc. B* **2010**, *365*, 699–712. [[CrossRef](#)]

18. Vannini, C.; Boscaro, V.; Ferrantini, F.; Benken, K.A.; Mironov, T.I.; Schweikert, M.; Gortz, H.-D.; Fokin, S.I.; Sabaneyeva, E.; Petroni, G. Flagellar movement in two bacteria of the family *Rickettsiaceae*: A re-evaluation of motility in an evolutionary perspective. *PLoS ONE* **2014**, *9*, e87718. [[CrossRef](#)]
19. Muñoz-Gómez, S.A.; Hess, S.; Burger, G.; Lang, B.F.; Susko, E.; Slamovits, C.H.; Roger, A.J. An updated phylogeny of the Alphaproteobacteria reveals that the parasitic Rickettsiales and Holosporales have independent origins. *eLife* **2019**, *8*, e42535. [[CrossRef](#)]
20. Sasser, D.; Lo, N.; Epis, S.; D'Auria, G.; Montagna, M.; Comandatore, F.; Horner, D.; Peretó, J.; Luciano, A.; Franciosi, F.; et al. Phylogenomic evidence for the presence of a flagellum and *cbb3* oxidase in the free-living mitochondrial ancestor. *Mol. Biol. Evol.* **2011**, *28*, 3285–3296. [[CrossRef](#)]
21. Fields, B.S.; Shotts, E.B.; Feeley, J.C.; Gorman, G.W.; Martin, W.T. Proliferation of *Legionella pneumophila* as an intracellular parasite of the ciliated protozoan *Tetrahymena pyriformis*. *Appl. Environ. Microbiol.* **1984**, *47*, 467–471. [[CrossRef](#)]
22. Barker, J.; Brown, M.R. Trojan horses of the microbial world: Protozoa and the survival of bacterial pathogens in the environment. *Microbiology* **1994**, *140*, 1253–1259. [[CrossRef](#)] [[PubMed](#)]
23. Ferrantini, F.; Fokin, S.I.; Vannini, C.; Modeo, L.; Verni, F.; Petroni, G. Ciliates as natural hosts of many novel *Rickettsia*-like bacteria. *Protistology* **2007**, *5*, 28–29.
24. Fokin, S.I.; Schrallhammer, M.; Chiellini, C.; Verni, F.; Petroni, G. Free-living ciliates as potential reservoirs for eukaryotic parasites: Occurrence of a trypanosomatid in the macronucleus of *Euplotes encysticus*. *Parasit. Vectors* **2014**, *7*, 203. [[CrossRef](#)] [[PubMed](#)]
25. Watanabe, K.; Nakao, R.; Fujishima, M.; Tachibana, M.; Shimizu, T.; Watarai, M. Ciliate *Paramecium* is a natural reservoir of *Legionella pneumophila*. *Sci. Rep.* **2016**, *6*, 24322. [[CrossRef](#)]
26. Fokin, S.; Sabaneyeva, E. Euryhaline paramecia (*Ciliophora*, *Peniculina*) of the Barents and the White Sea and its endobionts. Ecology, Reproduction and Guards Bioresources of the Seas of Northern Europe. In Proceedings of the III All-Union Conference, Murmansk, USSR, 16–21 July 1990; pp. 139–141. (In Russian).
27. Smurov, A.; Fokin, S. Resistance of *Paramecium caudatum* infected with endonuclear bacteria *Holospora* against salinity impact. *Proc. Zool. Inst. RAS* **1998**, *276*, 175–178.
28. Fokin, S.I. Bacterial endocytobionts of *Ciliophora* and their interactions with the host cell. *Int. Rev. Cytol.* **2004**, *236*, 181–249.
29. Görtz, H.-D.; Fokin, S.I. Diversity of endosymbiotic bacteria in *Paramecium*. In *Endosymbionts in Paramecium*; Fujishima, M., Ed.; Microbiology Monographs; Springer: Berlin/Heidelberg, Germany, 2009; Volume 12, pp. 131–160. [[CrossRef](#)]
30. Boscaro, V.; Schrallhammer, M.; Benken, K.A.; Krenek, S.; Szokoli, F.; Berendonk, T.U.; Schweikert, M.; Verni, F.; Sabaneyeva, E.V.; Petroni, G. Rediscovering the genus *Lyticum multiflagellated* symbionts of the order *Rickettsiales*. *Sci. Rep.* **2013**, *3*, 3305. [[CrossRef](#)]
31. Gelei, J. Uj *Paramecium* szeged kornyekerol. *Paramecium nephridiatum* nov. sp. *Állat. Közlem.* **1925**, *22*, 121–162, (In Hungarian with German summary).
32. Fokin, S.I.; Stoeck, T.; Schmidt, H.J. Rediscovery of *Paramecium nephridiatum* Gelei, 1925 and its characteristics. *J. Eukaryot. Microbiol.* **1999**, *46*, 416–426. [[CrossRef](#)]
33. Fokin, S.I. Bacterial endobionts of the ciliate *Paramecium woodruffi*. III. Endobionts of the cytoplasm. *Tsitologia* **1989**, *31*, 964–969, (In Russian with English summary).
34. Skovorodkin, I.N. A device for immobilizing biological objects in the light microscope studies. *Tsitologia* **1990**, *32*, 301–302, (In Russian with English summary).
35. Szokoli, F.; Sabaneyeva, E.; Castelli, M.; Krenek, S.; Schrallhammer, M.; Soares, C.A.G.; Da Silva-Neto, I.D.; Berendonk, T.U.; Petroni, G. “*Candidatus Fokinia solitaria*”, a novel “stand-alone” symbiotic lineage of *Midichloriaceae* (*Rickettsiales*). *PLoS ONE* **2016**, *11*, e0145743. [[CrossRef](#)]
36. Fokin, S.I. *Paramecium* genus: Biodiversity, some morphological features and the key to the main morphospecies discrimination. *Protistology* **2010**, *6*, 227–235.
37. Petroni, G.; Dini, F.; Verni, F.; Rosati, G. A molecular approach to the tangled intrageneric relationships underlying phylogeny in *Euplotes* (*Ciliophora*, *Spirotrichea*). *Mol. Phylogenet. Evol.* **2002**, *22*, 118–130. [[CrossRef](#)]
38. Medlin, L.; Elwood, H.J.; Stickel, S.; Sogin, M.L. The characterization of enzymatically amplified eukaryotic 16S-like rRNA-coding regions. *Gene* **1988**, *7*, 491–499. [[CrossRef](#)]

39. Rosati, G.; Modeo, L.; Melai, M.; Petroni, G.; Verni, F. A multidisciplinary approach to describe protists: A morphological, ultrastructural, and molecular study on *Peritromus kahli* Villeneuve-Brachon, 1940 (*Ciliophora*, *Heterotrichea*). *J. Eukaryot. Microbiol.* **2004**, *51*, 49–59. [[CrossRef](#)]
40. Vannini, C.; Rosati, G.; Verni, F.; Petroni, G. Identification of the bacterial endosymbionts of the marine ciliate *Euplotes magnicirratu*s (*Ciliophora*, *Hypotrichia*) and proposal of «*Candidatus* Devosia euplotis». *Int. J. Syst. Evol. Microbiol.* **2004**, *54*, 1151–1156. [[CrossRef](#)]
41. Cole, J.R.; Wang, Q.; Cardenas, E.; Fish, J.; Chai, B.; Farris, R.J.; Kulam-Syed-Mohideen, A.S.; McGarrell, D.M.; Marsh, T.; Garrity, G.M.; et al. The Ribosomal Database Project: Improved Alignments and New Tools for rRNA Analysis. *Nucleic Acids Res.* **2008**, *40*, 141–145. [[CrossRef](#)] [[PubMed](#)]
42. Quast, C.; Pruesse, E.; Yilmaz, P.; Gerken, J.; Schweer, T.; Yarza, P.; Peplies, J.; Glöckner, F.O. The SILVA ribosomal RNA gene database project: Improved data processing and web-based tools. *Nucleic Acids Res.* **2013**, *41*, 590–596. [[CrossRef](#)]
43. Manz, W.; Amann, R.; Ludwig, W.; Wagner, M.; Schleifer, K.-H. Phylogenetic oligodeoxynucleotide probes for the major subclasses of proteobacteria: Problems and solutions. *Syst. Appl. Microbiol.* **1992**, *15*, 593–600. [[CrossRef](#)]
44. Amann, R.I.; Binder, B.J.; Olson, R.J.; Chisholm, S.W.; Devereux, R.; Stahl, D.A. Combination of 16S rRNA-targeted oligonucleotide probes with flow cytometry for analyzing mixed microbial populations. *Appl. Environ. Microbiol.* **1990**, *56*, 1919–1925. [[CrossRef](#)] [[PubMed](#)]
45. Nawrocki, E.P. Structural RNA Homology Search and Alignment Using Covariance Models. Ph.D. Thesis, Washington University in Saint Louis, School of Medicine, St. Louis, MO, USA, 2009.
46. Darriba, D.; Taboada, G.L.; Doallo, R.; Posada, D. jModelTest 2: More models, new heuristics and parallel computing. *Nat. Methods* **2012**, *9*, 772. [[CrossRef](#)]
47. Guindon, S.; Gascuel, O. A simple, fast, and accurate algorithm to estimate large phylogenies by maximum likelihood. *Syst. Biol.* **2003**, *52*, 696–704. [[CrossRef](#)] [[PubMed](#)]
48. FigTree. Available online: <http://tree.bio.ed.ac.uk/software/figtree/> (accessed on 8 May 2020).
49. Lanzoni, O.; Castelli, M.; Sabaneyeva, E.; Lebedeva, N.; Potekhin, A.; Petroni, G. Diversity and environmental distribution of the cosmopolitan endosymbiont “*Candidatus* Megaira”. *Sci. Rep.* **2019**, *9*, 1179. [[CrossRef](#)] [[PubMed](#)]
50. Boscaro, V.; Petroni, G.; Ristori, A.; Verni, F.; Vannini, C. “*Candidatus* Defluviella procrastinata” and “*Candidatus* Cyrtobacter zanobii”, two novel ciliate endosymbionts belonging to the “Midichloria clade”. *Microb. Ecol.* **2013**, *65*, 302–310. [[CrossRef](#)] [[PubMed](#)]
51. Görtz, H.-D.; Dieckman, J. Life cycle and infectivity of *Holospora elegans*, a micronucleus specific symbiont of *Paramecium caudatum* Ehrenberg. *Protistol* **1980**, *16*, 591–603.
52. Boscaro, V.; Fokin, S.I.; Schrallhammer, M.; Schweikert, M.; Petroni, G. Revised systematics of *Holospora*-like bacteria and characterization of “*Candidatus* Gortzia infective”, a novel macronuclear symbiont of *Paramecium jenningsi*. *Microb. Ecol.* **2013**, *65*, 255–267. [[CrossRef](#)]
53. Potekhin, A.; Schweikert, M.; Nekrasova, I.; Vitali, V.; Schwarzer, S.; Anikina, A.; Kaltz, O.; Petroni, G.; Schrallhammer, M. Complex life cycle, broad host range and adaptation strategy of the intranuclear *Paramecium* symbiont *Preeria caryophila* comb. Nov. *FEMS Microbiol. Ecol.* **2018**, *94*. [[CrossRef](#)]
54. Eschbach, E.; Pfannkuchen, M.; Schweikert, M.; Drutschmann, D.; Brümmer, F.; Fokin, S.; Ludwig, W.; Görtz, H.D. “*Candidatus* Paraholospora nucleivisitans”, an intracellular bacterium in *Paramecium sexaurelia* shuttles between the cytoplasm and the nucleus of its host. *Syst. Appl. Microbiol.* **2009**, *32*, 490–500. [[CrossRef](#)]
55. Szokoli, F.; Castelli, M.; Sabaneyeva, E.; Schrallhammer, M.; Krenek, S.; Doak, T.G.; Berendonk, T.U.; Petroni, G. Disentangling the taxonomy of *Rickettsiales* and description of two novel symbionts (“*Candidatus* Bealeia paramacronuclearis” and “*Candidatus* Fokinia cryptica”) sharing the cytoplasm of the ciliate protist *Paramecium biaurelia*. *Appl. Environ. Microbiol.* **2016**, *82*, 7236–7247. [[CrossRef](#)]
56. Dümmler, J.S.; Walker, D.H. *Rickettsiales*. In *Bergey’s Manual of Systematics of Archaea and Bacteria*; Whitman, W.B., Rainey, F., Kämpfer, P., Trujillo, M., Chun, J., De Vos, P., Hedlund, B., Dedyshed, S., Eds.; John Wiley & Sons, Ltd.: Hoboken, NJ, USA, 2015.
57. Yarza, P.; Yilmaz, P.; Pruesse, E.; Glöckner, F.O.; Ludwig, W.; Schleifer, K.H.; Whitman, W.B.; Euzéby, J.; Amann, R.; Rosselló-Móra, R. Uniting the classification of cultured and uncultured bacteria and archaea using 16S rRNA gene sequences. *Nat. Rev. Microbiol.* **2014**, *12*, 635–645. [[CrossRef](#)]

58. Barco, R.A.; Garrity, G.M.; Scott, J.J.; Amend, J.P.; Nealson, K.H.; Emerson, D. A genus definition for Bacteria and Archaea based on a standard genome relatedness index. *mBio* **2020**, *11*, e02475-19. [[CrossRef](#)]
59. Przyboś, E.; Barth, D.; Berendonk, T.U. *Paramecium sexaurelia*–intra-specific polymorphism and relationships with other *Paramecium aurelia* spp., revealed by cytochrome b sequence data. *Folia Biol.* **2009**, *58*, 55–60. [[CrossRef](#)] [[PubMed](#)]
60. Osellame, L.D.; Blacker, T.S.; Duchen, M.R. Cellular and molecular mechanisms of mitochondrial function. *Best Pract. Res. Clin. Endocrinol. Metab.* **2012**, *26*, 711–723. [[CrossRef](#)]
61. Garushyants, S.K.; Beliavskaia, A.Y.; Malko, D.B.; Logacheva, M.D.; Rautian, M.S.; Gelfand, M.S. Comparative genomic analysis of *Holospora* spp., intranuclear symbionts of *Paramecia*. *Front. Microbiol.* **2018**, *9*, 1–11. [[CrossRef](#)]
62. Fokin, S.I.; Schweikert, M.; Görtz, H.-D.; Fujishima, M. Bacterial endocytobionts of *Ciliophora*. Diversity and some interactions with the host. *Eur. J. Protistol.* **2003**, *39*, 475–480. [[CrossRef](#)]
63. Sasser, D.; Beninati, T.; Bandi, C.; Bouman, E.A.P.; Sacchi, L.; Fabbi, M.; Lo, N. “*Candidatus* Midichloria mitochondrii”, an endosymbiont of the tick *Ixodes ricinus* with a unique intramitochondrial lifestyle. *Int. J. Syst. Evol. Microbiol.* **2006**, *58*, 2535–2540. [[CrossRef](#)] [[PubMed](#)]
64. Tashyreva, D.; Prokopchuk, G.; Votýpka, J.; Yabuki, A.; Horák, A.; Lukeš, J. Life cycle, ultrastructure, and phylogeny of new diplomonads and their endosymbiotic bacteria. *mBio* **2018**, *9*, e02447-17. [[CrossRef](#)]
65. Takeshita, K.; Yamada, T.; Kawahara, Y.; Narihiro, T.; Ito, M.; Kamagata, Y.; Shinzato, N. Tripartite Symbiosis of an Anaerobic Scuticociliate with two Hydrogenosome-Associated Endosymbionts, a *Holospora*-related Alphaproteobacterium and a Methanogenic Archaeon. *Appl. Environ. Microbiol.* **2019**, *85*, e00854-19. [[CrossRef](#)]
66. Han, B.; Lin, C.C.J.; Hu, G.; Wang, M.C. ‘Inside Out’–a dialogue between mitochondria and bacteria. *FEBS J.* **2019**, *286*, 630–641. [[CrossRef](#)]
67. Ratzka, C.; Gross, R.; Feldhaar, H. Endosymbiont tolerance and control within insect hosts. *Insects* **2012**, *3*, 553–572. [[CrossRef](#)] [[PubMed](#)]
68. Fisher, R.; Henry, L.; Cornwallis, C.; Kiers, E.T.; West, S.A. The evolution of host-symbiont dependence. *Nat. Commun.* **2017**, *8*, 15973. [[CrossRef](#)] [[PubMed](#)]



© 2020 by the authors. Licensee MDPI, Basel, Switzerland. This article is an open access article distributed under the terms and conditions of the Creative Commons Attribution (CC BY) license (<http://creativecommons.org/licenses/by/4.0/>).